



ELSEVIER

Contents lists available at ScienceDirect

Materials Letters

journal homepage: www.elsevier.com/locate/matlet

Phase transitions during high pressure torsion of Cu–Co alloys



B.B. Straumal^{a,b,c,d,*}, A.R. Kilmametov^{c,e}, Y. Ivanisenko^c, L. Kurmanaeva^{c,f}, B. Baretzky^c,
Y.O. Kucheev^{a,b,c}, P. Zięba^g, A. Korneva^g, D.A. Molodov^h

^a Institute of Solid State Physics, Russian Academy of Sciences, Ac. Ossipyan str. 2, 142432 Chernogolovka, Moscow, Russia

^b Laboratory of Hybrid Nanomaterials, National University of Science and Technology "MISIS", Leninskii prosp. 4, 119049 Moscow, Russia

^c Karlsruhe Institut für Technologie, Institut für Nanotechnologie, Hermann-von-Helmholtz-Platz 1, 76344 Eggenstein-Leopoldshafen, Germany

^d Moscow Institute of Physics and Technology (State University), Institutskii per. 9, 141700 Dolgoprudny, Russia

^e Institute of Physics of Advanced Materials, Ufa State Aviation Technical University, K. Marx St. 12, 450000 Ufa, Russia

^f Department of Chemical Engineering & Materials Science, University of California, One Shields Avenue, Davis, CA 95616, USA

^g Institute of Metallurgy and Materials Science, Polish Academy of Sciences, Reymonta St. 25, 30-059 Cracow, Poland

^h Institute of Physical Metallurgy and Metal Physics, RWTH Aachen University, Kopernikusstr. 14, 52056 Aachen, Germany

ARTICLE INFO

Article history:

Received 11 November 2013

Accepted 10 December 2013

Available online 18 December 2013

Keywords:

Severe plastic deformation

Precipitation

Dissolution

Steady-state

Phase transformations

ABSTRACT

High-pressure torsion of Cu–4.9 wt% Co alloy has been studied, with Co fully dissolved in the Cu matrix and fully precipitated from the matrix. A steady-state was reached in both samples after 1–2 anvil rotations. The solid solution in the first sample partly decomposed. The Co precipitates in the second sample partly dissolved in the matrix. In both cases the Co precipitates surrounded by the Cu-based solid solution with about 2.5 wt% Co were formed.

© 2013 Elsevier B.V. All rights reserved.

1. Introduction

Severe plastic deformation (SPD) always induces grain refinement in materials and frequently leads to phase transformations [1,2]. Thus, SPD can induce the dissolution of phases [3,4], formation [5] or decomposition [6] of a supersaturated solid solution, disordering of ordered phases [7], amorphization of crystalline phases [8,9], synthesis of the low-temperature [10], high-temperature [11] or high-pressure [12,13] allotropic modifications, and nanocrystallization in the amorphous matrix [14]. The phases forming in the steady-state during SPD can also appear after long annealing at a certain temperature T_{eff} with subsequent quenching [2,3,6–8]. In equilibrium, the phases in the material are fully defined by the respective point in the equilibrium phase diagram and do not depend on the starting state before annealing. Does the composition of phases in the steady-state during SPD depend on the amount and structure of phases before SPD, or are these phases *equifinal* i.e. independent on the starting state [15]? (We suppose here that SPD processing is done under the given conditions.) To answer this question the Cu–4.9 wt% Co alloy has been chosen. Two different states were subjected to high

pressure torsion, namely with Co fully dissolved in and fully precipitated from the Cu matrix.

2. Experimental

The Cu–4.9 wt% Co alloy has been prepared from high-purity 5N Cu and Co by vacuum induction melting into cylindrical ingots. For HPT processing, the 0.6 mm thick discs were cut from the as-cast ingots, then ground and chemically etched. They were sealed into evacuated silica ampoules with a residual pressure of approximately 4×10^{-4} Pa at room temperature. Samples were annealed at 570 °C for 840 h (Sample 1) and at 1060 °C for 10 h (Sample 2), and then quenched in water. The accuracy of the annealing temperature was ± 1 °C. The annealed samples were subjected to HPT at room temperature under a pressure of 5 GPa in a Bridgman anvil-type unit (1 and 5 rotations of the anvil with the rate of 1 rpm). Samples for microstructural and X-rays investigations were cut from the HPT-processed discs at a distance of 3 mm from the sample center. Transmission electron microscopy (TEM) investigations were carried out using a TECNAI FEI, G2 FEG microscope at an accelerating voltage of 200 kV. Scanning electron microscopy (SEM) investigations were carried out on a Philips XL30 scanning microscope equipped with a LINK ISIS energy-dispersive X-ray spectrometer produced by Oxford Instruments. X-ray diffraction (XRD) data were obtained on a Pan Analytical

* Corresponding author at: Institute of Solid State Physics, Russian Academy of Sciences, Ac. Ossipyan str. 2, 142432 Chernogolovka, Moscow, Russia.

Tel.: +7 916 6768673; fax: +7 499 2382326.

E-mail address: straumal@issp.ac.ru (B.B. Straumal).

X'Pert (Philips) diffractometer (Cu K α radiation). Lattice parameter values were estimated using the powder diffraction tool of "Fityk software" [16].

3. Results and discussion

The as cast Cu–4.9 wt% Co alloy contained grains of Cu-based solid solution (with grain size 10–20 μm), Co particles with size about 2 μm and fine dispersed Co precipitates with a size about 10–20 nm [17]. Co fully dissolved into Cu after annealing at 1060 $^{\circ}\text{C}$ for 10 h (sample 2) because the solubility of Co in Cu at 1060 $^{\circ}\text{C}$ is about 8 wt% Co [18]. The grain size after this annealing was about 50 μm . During annealing at 570 $^{\circ}\text{C}$ for 840 h (Sample 1), the Cu-based solid solution almost fully decomposed; less than 0.5 wt% Co remained dissolved in Cu (based on XRD measurements and phase diagram [18]). The grain size of Cu grains was about 20 μm , that of large Co precipitates in Cu/Cu grain boundaries was about 5 μm and that of fine Co precipitates in Cu grains was about 50 nm (insets in Fig. 1a). After HPT of both samples the Cu grain size drastically decreased to about 200 nm, and all Co-precipitates to only 10–20 nm (insets in Fig. 1b). The last value was evaluated from the XRD data [17]. Cu grains are nearly equiaxial; the Co-particles are uniformly distributed among Cu grains. The steady-state grain size during HPT of pure Cu was 80–120 nm [19].

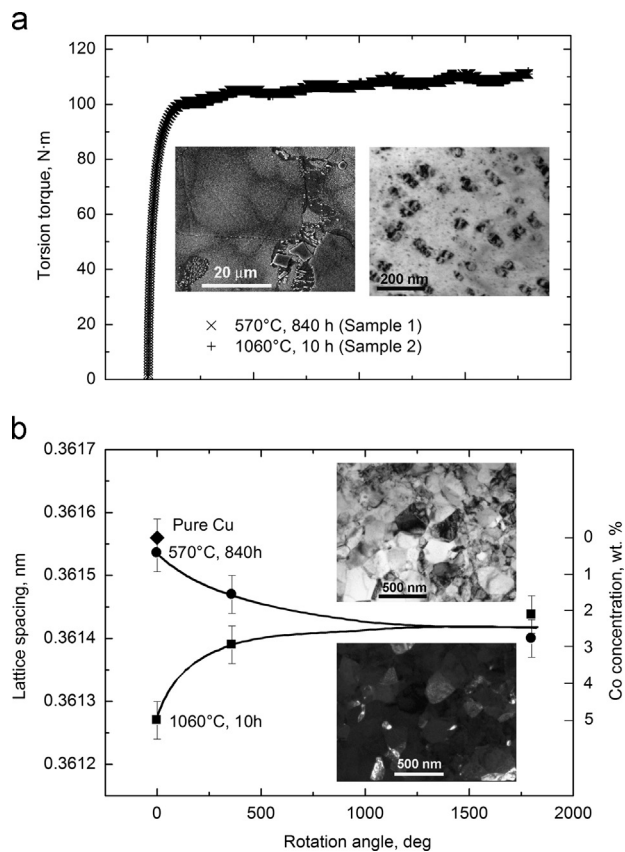


Fig. 1. (a) Dependence of torsion torque on the rotation angle. Insets: SEM (left) and bright-field TEM (right) micrographs of Cu–4.9 wt% Co alloy after annealing at 570 $^{\circ}\text{C}$ for 840 h. (b) Dependence of lattice spacing on the rotation angle. Circles mark the lattice spacing in Sample 1 annealed at 570 $^{\circ}\text{C}$ for 840 h. Squares correspond to the Sample 2 annealed at 1060 $^{\circ}\text{C}$ for 10 h. Diamond shows the lattice spacing for pure copper. The respective Co concentration is shown on the right vertical axis. Insets: bright-field (top) and dark-field (bottom) TEM micrographs of Cu–4.9 wt% Co alloy after annealing at 570 $^{\circ}\text{C}$ for 840 h and HPT (6 GPa, 5 rot, 1 rpm).

Fig. 1a shows the dependence of torsion torque on the rotation angle (strain). After short work hardening during the first rotation of the anvils, the torsion torque in both samples reaches steady-state and remains almost constant. Fig. 1b shows the dependence of the lattice parameter in Sample 1 annealed at 570 $^{\circ}\text{C}$ for 840 h (circles) and Sample 2 annealed at 1060 $^{\circ}\text{C}$ for 10 h (squares) on the rotation angle. The lattice parameter of Sample 1 before deformation is very close to that of pure copper (diamond). With an increasing number of rotations, the lattice parameter of Sample 1 decreased and that of Sample 2 increased. After 5 anvil rotations (1800 $^{\circ}$) the lattice parameter in both samples becomes almost undistinguishable and corresponds to the solid solution of Co in Cu with 2.5 wt%. In other words, the composition of the solid solution in the Cu–4.9 wt% Co alloy after the given HPT processing does not depend on the initial state prior to HPT. Thus, the steady-state with respect to the grain size, size of Co precipitates and concentration of Co in a solid solution during HPT is indeed *equifinal*.

The composition of Cu-rich matrix in both alloys before and after HPT is shown in the Cu–Co phase diagram (Fig. 2). The solid solution in Samples 1 and 2 after HPT contains as much Co, as if they would be annealed at $T_{\text{eff}1} = 920 \pm 30$ $^{\circ}\text{C}$ and $T_{\text{eff}2} = 870 \pm 30$ $^{\circ}\text{C}$, respectively.

As described above, the Co precipitates in Sample 1 were partly dissolved during HPT, which was accomplished in a period of time of $t = 300$ s. Let us suppose that this dissolution was controlled by the atomic diffusion. The diffusion path in this case would be equal to the distance between fine Co precipitates in Sample 1, i.e. $d = 200$ nm (right inset in Fig. 1a). It corresponds to the bulk diffusion coefficient of $D = 10^{-16}$ m^2/s . On the other hand, the extrapolation of the published results of diffusion measurements to the temperature of the current

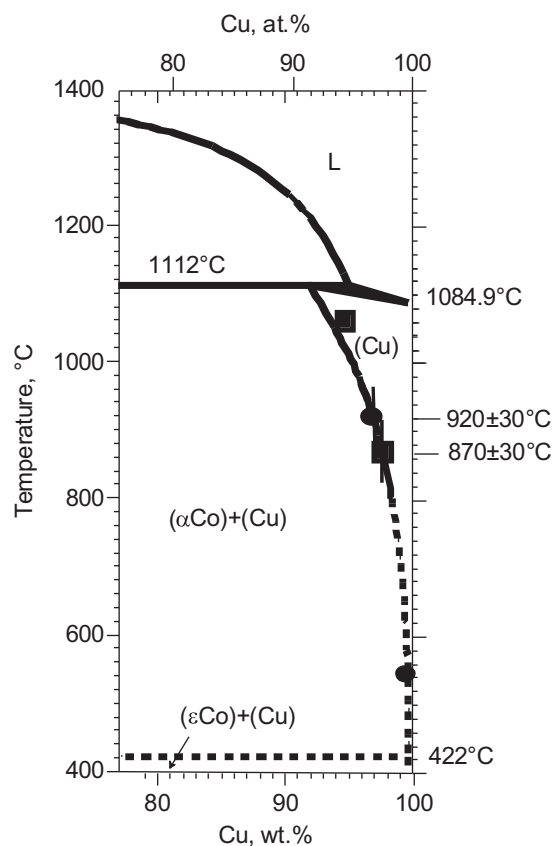


Fig. 2. The Cu-rich part of the Co–Cu phase diagram [18]. The composition of Cu-rich matrix in both alloys before and after HPT is shown. Circles mark the data for Sample 1 annealed before HPT at 570 $^{\circ}\text{C}$. Squares correspond to the Sample 2 annealed before HPT at 1060 $^{\circ}\text{C}$.

SPD treatment, T_{SPD} , $T_{SPD}=300$ K gives $D=10^{-38}$ m²/s for diffusion of Co in Cu [20] and $D=10^{-35}$ m²/s for self-diffusion in Cu [21]. If we suppose that the mass transfer was controlled by the grain boundary (GB) diffusion, the extrapolation of the respective data to T_{SPD} reveals $D_{GB}=10^{-19}$ m²/s for Cu self-diffusion [22], $D_{GB}=10^{-22}$ m²/s for Ni GB diffusion in coarse-grained Cu polycrystals [23] and $D_{GB}=10^{-19}$ m²/s for Ni GB diffusion in nanograined Cu polycrystals [24] (D_{GB} for Co was not measured up to now). As seen, the discrepancy is high; the mass transfer during SPD (HPT in the current work) occurs from 3 to 12 orders of magnitude faster than any possible diffusion process can facilitate. Moreover, the applied pressure of 6 GPa additionally slows down the diffusion as well as GB migration [25–27]. Therefore, we have to consider the deformation-driven mechanisms of mass transfer.

For analysis of the obtained results the model developed for the interpretation of the SPD-driven dissolution of cementite precipitates in steel [28] can be applied. The authors of Ref. [28] assumed that during HPT a relatively soft matrix flows around the harder precipitates. Due to the friction at the precipitate/matrix interface this results in a high elastic strain in the precipitates and leads to wear (abrasion) of the precipitates. The difference of deformation γ of both phases in the present case of almost pure shear takes the form $\gamma_{Cu}/\gamma_{Co}=p$ [28]. Since the shear and Young's moduli of Co are about two times higher than those of Cu [29], $p=0.5$. It is higher than $p=0.2$ in case of cementite in steel but is sufficient to consider the wear mechanism. In such a case the travel distance relative to the Co particle would be equal to $x_{wear}=(1-p)\lambda\gamma$, where λ is the precipitate size [28]. The shear strain γ after one anvil rotation is $\gamma=64$ [28], $\lambda=50$ nm (right inset in Fig. 1a) and $x_{wear}=1600$ nm. Therefore, the wear mechanism is sufficient for the mass transfer both in Samples 1 and 2. After a certain strain, the "stream" in the copper matrix surrounding a Co precipitate already contains the Co atoms. In the steady-state the dissolution of Co atoms in the stream and precipitation from the stream are equal, and a certain steady-state concentration of cobalt in copper should be obtained.

The SPD-driven phase transformations can also be analyzed while assuming [30] that the steady-state concentration of lattice defects during SPD is higher than that in the equilibrium at the temperature of SPD-treatment, T_{SPD} , and pressure of the SPD-treatment, p_{SPD} . This concentration would be equal to the equilibrium concentration of lattice defects at a certain effective temperature T_{eff} [2]. In our case T_{eff} amounts to $T_{eff}=900$ °C (Fig. 2). The extrapolation of bulk diffusion coefficients to T_{eff} gives $D=5 \cdot 10^{-14}$ m²/s for diffusion of Co in Cu [20] and $D=10^{-13}$ m²/s for self-diffusion in Cu [21]. Indeed, the deformation driven mechanisms can ensure the mass-transfer rate which is comparable with the bulk diffusion fluxes at $T_{eff}=900$ °C. The bulk diffusion fluxes at 900 °C could ensure the decomposition/precipitation rates even if the effect of pressure is taken into account.

The existence of steady-state during HPT suggests that the production rate of the deformation-induced lattice defects (e.g. multiplication of dislocations or vacancy production by the recombination of dislocations [31,32]) is equal to the relaxation rate of these defects. Such a process resembles the dynamic recovery and recrystallization during high-temperature deformation (for example in power plant steels) [33]. However, at high temperatures the defect relaxation occurs by bulk and grain boundary diffusion. In the current case of HPT at the ambient temperature of 300 K, as discussed above, the diffusion is very slow. It can be, therefore, supposed that not only producing the defects but also their relaxation is strain/stress-driven. A possible mechanism explaining such a relaxation is the motion of grain boundaries. As was predicted theoretically [34,35], corroborated by computer simulations [35,36], observed in TEM investigations of sole boundaries in nanocrystalline and ultra-fine grained polycrystals [37] and unambiguously proven in experiments on bicrystals [38–41], grain boundaries can be driven

by an applied stress and this motion is coupled to the shear strain of the crystals region behind the moving boundary. Therefore, our understanding of the observed steady-state (with respect to the production and relaxation of the deformation induced microstructural defects) is that a substantial amount of deformation during HPT of the investigated specimens was accommodated by grain boundary migration, which in turn is associated with an annihilation and/or absorption of dislocations and excess vacancies in the grain interiors swept by the boundaries. Taking into account the huge shear deformation of a specimen (with a diameter of 10 mm) already after 360° of anvil rotation during HPT and assuming the coupling factor β between the normal boundary displacement and lateral grain translation to be in the range between 0.1 and 1 [35,40], it can be easily seen that even for the boundaries with β close to 0.1 the corresponding total migration distance can be compared with the sample thickness of 0.4 mm.

4. Conclusions

To conclude, we reported on the experimental evidence that the steady state with respect to the grain size, size of precipitates and the composition of a solid solution in a Cu–4.9 wt% Co alloy during HPT is *equifinal*. The experiments revealed that HPT of Cu-based solid solution with 4.9 wt% Co led to its partial decomposition and precipitation of Co, whereas HPT of almost pure Cu containing Co particles resulted in their partial dissolution. Thus, the final state of the Cu–4.9 wt% Co alloy after HPT does not depend on the initial microstructure/composition, the Cu-rich matrix contained about 2.5 wt% Co. It is equivalent to the concentration of Co in a Cu–Co solid solution after annealing at a temperature of about 900 °C.

Acknowledgments

The work was partially supported by the Russian Foundation for Basic Research (Grants 11-03-01198 and 13-08-90422), the Russian Federal Ministry for Education and Science (Grant 14.A12.31.0001), the EraNet.Rus programme (Grant STProjects-219) and Karlsruhe Nano Micro Facility. TEM and SEM studies were supported by the Polish National Science Centre (Grant DEC-2011/01/M/ST8/07822). One of the authors (DM) expresses his gratitude to the Deutsche Forschungsgemeinschaft for financial support (Grant MO 848/14).

References

- [1] Sauvage X, Chbihi A, Quelelennec X. *J Phys* 2010;240:012003.
- [2] Straumal BB, Mazilkin AA, Baretzky B, Rabkin E, Valiev RZ. *Mater Trans* 2012;53:63–71.
- [3] Straumal BB, Dobatkin SV, Rodin AO, Protasova SG, Mazilkin AA, Goll D, et al. *Adv Eng Mater* 2011;13:463–9.
- [4] Sauvage X, Ivanisenko Y. *J Mater Sci* 2007;42:1615–21.
- [5] Sauvage X, Jessner P, Vurpillot F, Pippan R. *Scr Mater* 2008;58:1125–8.
- [6] Straumal BB, Baretzky B, Mazilkin AA, Philipp F, Kogtenkova OA, Volkov MN, et al. *Acta Mater* 2004;52:4469–78.
- [7] Korznikov AV, Tram G, Dimitrov O, Korznikova GF, Idrisova SR, Pakiela Z. *Acta Mater* 2001;49:663–71.
- [8] Prokoshkin SD, Khmelevskaya IYu, Dobatkin SV, Trubitsyna IB, Tatyaniyev EV, Stolyarov VV, et al. *Acta Mater* 2005;53:2703–14.
- [9] Sauvage X, Renaud L, Deconihout B, Blavette D, Ping DH, Hono K. *Acta Mater* 2001;49:389–94.
- [10] Sagaradze VV, Shabashov VA. *Nanostruct Mater* 1997;9:681–4.
- [11] Ivanisenko Yu, MacLaren I, Sauvage X, Valiev RZ, Fecht H-J. *Acta Mater* 2006;54:1659–69.
- [12] Pérez-Prado MT, Zhilyaev AP. *Phys Rev Lett* 2009;102:175504.
- [13] Ivanisenko Yu, Kilmametov A, Rösner H, Valiev RZ. *Int J Mat Res* 2008;1:36–41.
- [14] Kovács Zs, Henits P, Zhilyaev AP, Révész Á. *Scr Mater* 2006;54:1733–7.
- [15] von Bertalanffy L. *Hum Biol* 1951;23:302–12.
- [16] Wojdyr M. *J Appl Cryst* 2010;43:1126–8.

- [17] Straumal BB, Protasova SG, Mazilkin AA, Kogtenkova OA, Kurmanaeva L, Baretzky B, et al. *Mater Lett* 2013;98:217–21.
- [18] Massalski TB, Murray JL, Bennett LH, Baker H, Kacprzak BP, Burton TB, et al., editors. *Materials Park*: ASM International; 1993.
- [19] Kilmametov AR, Vaughan G, Yavari AR, LeMoulec A, Botta WJ, Valiev RZ. *Mater Sci Eng A* 2009;503:10–3.
- [20] Mackliet CA. *Phys Rev* 1958;109:1964–70.
- [21] Fujikawa S, Hirano KI. In: *Proceedings of the Yamada Vth conference on point defects, defect interactions in metals*, Takamura JI, Doyama M, Kiritani M, editors. University of Tokyo Press; 1982. p. 554–8.
- [22] Surholt T, Herzig Chr. *Acta Mater* 1997;45:3817–23.
- [23] Divinski S, Ribbe J, Schmitz G, Herzig Chr. *Acta Mater* 2007;55:3337–46.
- [24] Amouyal Y, Divinski SV, Estrin Y, Rabkin E. *Acta Mater* 2007;55:5968–79.
- [25] Straumal BB, Klinger LM, Shvindlerman LS. *Scr Metall* 1983;17:275–9.
- [26] Molodov DA, Straumal BB, Shvindlerman LS. *Scr Metall* 1984;18:207–11.
- [27] Molodov DA, Swiderski J, Gottstein G, Lojkowski W, Shvindlerman LS. *Acta Metall Mater* 1994;42:3397–407.
- [28] Ivanisenko Yu, Lojkowski W, Valiev RZ, Fecht H-J. *Acta Mater* 2003;51:5555–70.
- [29] Soboyejo WO, editor. Boca Raton, FL: CRC Press; 2007.
- [30] Martin G. *Phys Rev B* 1984;30:1424–36.
- [31] Friedel J. *Dislocations*. Oxford: Pergamon Press; 1964.
- [32] Ungár T, Schaffler E, Hanák P, Bernstorff S, Zehetbauer M. *Mater Sci Eng A* 2007;462:398–401.
- [33] Doherty RD, Hughes DA, Humphreys FJ, Jonas JJ, Juul Jensen D, Kassner ME, et al. *Mater Sci Eng A* 1997;238:219–74.
- [34] Read WT, Shockley W. *Phys Rev* 1950;78:275–89.
- [35] Cahn JW, Mishin Y, Suzuki A. *Acta Mater* 2006;54:4953–75.
- [36] Elsener A, Politano O, Derlet PM, van Swygenhoven H. *Acta Mater* 2009;57:1988–2001.
- [37] Momprou F, Caillard D, Legros M. *Acta Mater* 2009;57:2198–209.
- [38] Sheikh-Ali AD, Lavrentyev FF, Kazarov YuG. *Acta Mater* 1997;45:4505–12.
- [39] Molodov DA, Ivanov VA, Gottstein G. *Acta Mater* 2007;55:1843–8.
- [40] Gorkaya T, Molodov DA, Gottstein G. *Acta Mater* 2009;57:5396–405.
- [41] Gorkaya T, Molodov KD, Molodov DA, Gottstein G. *Acta Mater* 2011;59:5674–80.